Raman Spectroscopic Study on the Copper(II) Binding Mode of Prion Octapeptide and Its pH Dependence†

Takashi Miura, Ayako Hori-i, Hideyuki Mototani, and Hideo Takeuchi*

Graduate School of Pharmaceutical Sciences, Tohoku University, Aobayama, Sendai 980-8578, Japan

Received April 26, 1999; Revised Manuscript Received June 14, 1999

ABSTRACT: The cellular form of prion protein is a precursor of the infectious isoform, which causes fatal neurodegenerative diseases through intermolecular association. One of the characteristics of the prion protein is a high affinity for Cu(II) ions. The site of Cu(II) binding is considered to be the N-terminal region, where the octapeptide sequence PHGGGWGQ repeats 4 times in tandem. We have examined the Cu(II) binding mode of the octapeptide motif and its pH dependence by Raman and absorption spectroscopy. At neutral and basic pH, the single octapeptide PHGGGWGQ forms a 1:1 complex with Cu(II) by coordinating via the imidazole N_π atom of histidine together with two deprotonated main-chain amide nitrogens in the triglycine segment. A similar 1:1 complex is formed by each octapeptide unit in $(PHGGGWGQ)_2$ and $(PHGGGWGQ)_4$. Under weakly acidic conditions (pH ∼ 6), however, the Cu(II)−amide$^-$ linkages are broken and the metal binding site of histidine switches from N_π to N_τ to share a Cu(II) ion between two histidine residues of different peptide chains. The drastic change of the Cu(II) binding mode on going from neutral to weakly acidic conditions suggests that the micro-environmental pH in the brain cell regulates the Cu(II) affinity of the prion protein, which is supposed to undergo pH changes in the pathway from the cell surface to endosomes. The intermolecular His(N_τ)−Cu(II)−His(N_τ) bridge may be related to the aggregation of prion protein in the pathogenic form.

The prion protein (PrP)[1] is a glycolipid-anchored cell surface protein which is expressed mainly in the central nervous system (*1*, *2*). The lack of PrP causes extensive loss of cerebellar Purkinje cells (*3*) and alteration of both circadian activity rhythms and sleep pattern (*4*). The cellular isoform of PrP (PrP^C) undergoes a conformational transition from α-helix-rich to β-sheet-rich structure under unknown conditions, and abnormal aggregation of the β-sheet-rich isoform, PrP^{Sc}, causes fatal neurodegenerative diseases including Creutzfeldt−Jakob disease in human and spongiform encephalopathy in animals (*1*, *5*, *6*). The physiological function of PrP^C and the mechanism of the formation of pathogenic PrP^{Sc} remain unclear despite intensive biochemical and biophysical studies.

Mature mammalian PrP^C after posttranslational modifications spans residues 23−231 of the 253-amino acid sequence coded by a single gene (*7*−*9*). The C-terminal region (residues 121−231) of PrP^C forms a globular structure comprising three α-helices and two short β-strands, while the N-terminal region (23−120) is highly flexible (*10*, *11*). The N-terminal region of human PrP^C contains four repeats of the octapeptide Pro-His-Gly-Gly-Gly-Trp-Gly-Gln (PHGGGWGQ) at positions 60−91 with an analogous nonapeptide, PQGGGGWGQ, on the adjacent N-terminal side (residues 51−59). The octapeptide and its repeats are also found in animals (*12*) and have high affinities for divalent metal ions, in particular for Cu(II) (*13*, *14*). The Cu content in brains from PrP^C gene-ablated ($Prnp^{0/0}$) mice is significantly lowered compared to that in wild-type mouse brains (*15*). These findings have raised the possibility that PrP^C is involved in the transport of Cu(II) into brain cells and the octapeptide repeat region plays a role in Cu(II) binding.

Equilibrium dialysis studies have provided information on the stoichiometry of Cu(II) binding of PrP^C. Brown et al. have shown that the N-terminal region of PrP^C possesses five to six binding sites for Cu(II) (*15*), which is consistent with the previous finding that one octapeptide unit can bind one Cu(II) ion (*15*, *16*). On the other hand, Stöckel et al. have demonstrated that full-length PrP^C has only two Cu(II) binding sites (*14*). According to the model proposed by Stöckel et al., histidyl imidazole nitrogens of two octapeptide units cooperatively bind a single Cu(II) ion. Very recently, Viles et al. have examined the Cu(II) binding properties of peptides containing 2−4 repeats of the octapeptide motif by circular dichroism, absorption, electron spin resonance, and nuclear magnetic resonance spectroscopy (*17*). To explain the observed binding properties, they have proposed a model in which Cu(II) ions are coordinated by the main-chain amide nitrogens of histidine residues as well as by histidyl imidazole nitrogens.

† This work was supported in part by a Grant-in-Aid (09780593) from the Ministry of Education, Science, Sports, and Culture of Japan and by the Association for the Progress of New Chemistry (ASPRONC) Foundation.

* Corresponding author. Phone/FAX: +81-22-217-6855. Email: takeuchi@mail.cc.tohoku.ac.jp.

[1] Abbreviations: PrP, prion protein; PrP^C, normal cellular isoform of PrP; PrP^{Sc}, pathogenic isoform of PrP; OP1, octapeptide PHGGGWGQ; OP2, 16-mer peptide $(PHGGGWGQ)_2$; OP4, 32-mer peptide $(PHGGGWGQ)_4$; *r*, molar concentration ratio of the Cu(II) ion to the octapeptide unit.

10.1021/bi9909389 CCC: $18.00
Published on Web 08/12/1999

In this study, we have examined Raman and absorption spectra of the octapeptide and its repeats in the presence of varied concentrations of Cu(II). Raman spectroscopy is a useful tool to investigate the Cu(II) binding site on the histidyl imidazole ring and to detect the deprotonation of amide nitrogens associated with the formation of Cu(II)−amide linkages. On the other hand, absorption spectroscopy can be used to detect changes of the ligands coordinating to the Cu(II). Analysis of the observed Raman and absorption spectra has shown that each octapeptide unit binds one Cu(II) ion via the N_π atom of histidine and two deprotonated amide nitrogens of the neighboring triglycine segment at neutral and basic pH. At weakly acidic pH, however, the amide nitrogens dissociate from the Cu(II), and the site of Cu(II) binding on the imidazole ring changes from N_π to N_τ. The drastic change of the binding mode results in the formation of a 1:2 Cu(II)−octapeptide complex and facilitates intermolecular association through His(N_τ)−Cu(II)−His(N_τ) bridges.

EXPERIMENTAL PROCEDURES

Materials. The pentapeptide PHGGG, the octapeptide PHGGGWGQ (OP1), and tandem repeats of the octapeptide unit, $(PHGGGWGQ)_2$ (OP2) and $(PHGGGWGQ)_4$ (OP4), were synthesized on an Applied Biosystems Model 431A automated peptide synthesizer by using the 9-fluorenylmethoxycarbonyl (Fmoc) method. The N-terminal Pro was acetylated in order to avoid deprotonation and metal coordination of the imino nitrogen. Cleavage of the peptide from the resin and removal of protecting groups from the peptide were performed in a mixture of 10 mL of trifluoroacetic acid, 0.75 g of phenol, 0.25 mL of dithioethylene glycol, 0.5 mL of thioanisole, and 0.5 mL of water. The crude peptide was purified by HPLC on a reversed-phase column (Cosmosil $5C_{18}$-AR) by using a 0−50% linear gradient of acetonitrile in 0.1% (v/v) trifluoroacetic acid. Lyophilized powder of the purified peptide was dissolved in 50 mM hydrochloric acid and again lyophilized to remove residual trifluoroacetic acid. Copper(II) chloride was purchased from Nacalai Tesque, Inc.

Preparation of Samples. Although the peptides were highly soluble at any pH in the absence of Cu(II), the solubilities of the peptides, in particular of OP2 and OP4, were significantly lowered around pH 6 in the presence of Cu(II). To minimize the effects of aggregation, the samples for spectral analysis were prepared under weakly alkaline conditions, pH (pD) 8.2, except for the samples used in pH (pD) dependence experiments. The peptide was dissolved in deionized H_2O or in D_2O (Isotec Inc.), and the pH (pD) of the sample solution was adjusted by adding a small amount of aqueous KOH (KOD). The concentration of PHGGG was determined from the Raman intensity of histidine using a predetermined standard curve of histidine Raman intensity versus concentration. For OP1, OP2, and OP4, the UV absorption intensity of the tryptophan residue (ϵ_{280} = 5460 M^{-1} cm^{-1}) was used to determine the concentration. Samples for Raman measurements contained 20 mM (PHGGG and OP1), 10 mM (OP2), or 5 mM (OP4) peptide (20 mM in octapeptide unit for the repeats). In examining the pH (pD) dependence of the structure of the Cu(II)−OP2 complex, aqueous KOH (KOD) or HCl (DCl) was used to adjust the pH (pD). At pH (pD) 6.0, an extensive precipitation was observed even at low concentrations of Cu(II), and therefore the Raman spectrum of Cu(II)−OP2 at this pH was obtained from the precipitated material.

The peptide concentration for visible absorption measurements was 120 μM for PHGGG. The same concentration (120 μM) in octapeptide unit was employed for OP1, OP2, and OP4. The pH of the solution was adjusted to 8.2 by adding aqueous KOH. No precipitation was observed in the highly diluted solutions except for OP4.

Raman and Visible Absorption Spectroscopy. Raman spectra were excited with the 514.5-nm line (40 mW at the sample) of a Coherent Innova 70 Ar^+ laser and were recorded on a Jasco NR-1800 triple spectrometer equipped with a liquid-nitrogen-cooled CCD detector. Wavenumber calibration was effected by using the indene Raman spectrum, and the wavenumbers of sharp Raman bands were reproducible to within ±0.5 cm^{-1}. The intensities of Raman spectra were normalized by using the 1640 cm^{-1} band of H_2O or the 1210 cm^{-1} band of D_2O for PHGGG solutions. For OP1, OP2, and OP4, the strongest Raman band of tryptophan at 1552 cm^{-1} was used as an intensity standard. The solvent Raman bands were subtracted after the intensity normalization. Visible absorption spectra were recorded on a Hitachi U-3300 spectrophotometer using a quartz optical cell of 5-cm path length. Samples were kept at 22 °C during the collection of Raman and absorption spectra.

RESULTS

Raman Spectra of Cu(II)−PHGGG. The pentapeptide PHGGG corresponds to the N-terminal segment of the octapeptide of PrP, PHGGGWGQ, and may be directly involved in the binding of Cu(II) (*16*). In the left panel of Figure 1, we show the Raman spectra of H_2O solutions (pH 8.2) of PHGGG at Cu(II)/peptide molar ratios (r) of 0, 0.5, and 1.0. The broad band around 1665 cm^{-1} is assigned to the amide I vibration of the peptide backbone. Some of the other bands in the spectra are ascribed to vibrations of the imidazole side chain of histidine. A pair of bands at 1587 (shoulder) and 1574 cm^{-1} in the spectrum at $r = 0$ are assigned to the $C_4{=}C_5$ stretching vibration of the histidyl imidazole ring of two tautomeric forms, either N_π- or N_τ-protonated, respectively (*18*) (see Figure 2). The $C_4{=}C_5$ stretch bands decrease in intensity upon Cu(II) binding (Figure 1B) and almost disappear at $r = 1.0$ (Figure 1C). Concomitantly, a band appears at 1590 cm^{-1}, which is assignable to the $C_4{=}C_5$ stretch of metal-bound histidine (*16*). The wavenumber of the $C_4{=}C_5$ stretch band of metal-bound histidine is sensitive to the site of metal binding: 1580 ± 10 cm^{-1} in the N_π−metal form and 1600 ± 6 cm^{-1} in the N_τ−metal form (*19*, *20*) (see Figure 2). According to this relationship, the appearance of the 1590 cm^{-1} band at r = 0.5 and 1.0 indicates that Cu(II) binds to the histidyl N_π atom.

The 1272 cm^{-1} band of the metal-free peptide (Figure 1A) is assigned to the imidazole ring breathing mode of histidine (*18*), which may be partly overlapped by the amide III band of the peptide main chain. Upon Cu(II) binding, this band exhibits a significant intensity increase (Figure 1, B and C). This observation is consistent with the previous finding that the imidazole ring breathing mode gains intensity when a metal ion binds to the N_π atom but not to the N_τ atom (*19*).

The hydrogen atom attached to the N_π or N_τ atom of histidine readily exchanges with deuterium in D_2O solution.

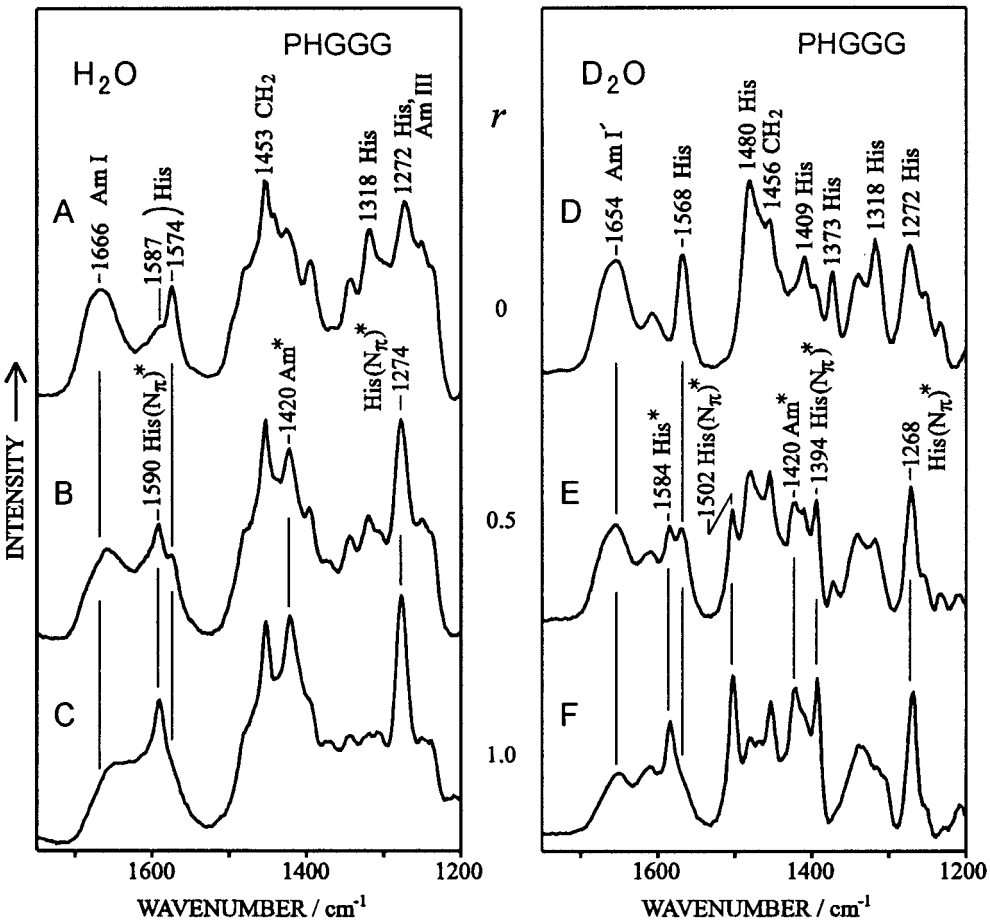

FIGURE 1: Raman spectra of H_2O (left panel) and D_2O (right panel) solutions of pentapeptide PHGGG [20 mM, pH (pD) 8.2] at varied $CuCl_2$ concentrations. The molar concentration ratio of Cu(II) to peptide (*r*) increases from top to bottom: 0 (A and D), 0.5 (B and E), and 1.0 (C and F). The Raman intensities of the spectra were normalized by using the solvent (H_2O or D_2O) Raman band, which was subtracted after the intensity normalization. The assignments of Raman bands are indicated as follows: His, metal-free histidine; His(N_π)*, histidine bound to Cu(II) via N_π; His*, histidine bound to Cu(II) via either N_π or N_τ; Am I, amide I; Am I′, amide I′; Am III, amide III; Am*, deprotonated amide bound to Cu(II); CH_2, methylene.

As a result, the $C_4{=}C_5$ stretch vibration becomes insensitive to the tautomerism and gives a singlet Raman band around 1570 cm^{-1}, though a wavenumber upshift of the $C_4{=}C_5$ stretch band upon metal binding still occurs for N-deuterated histidine (*19*). In the right panel of Figure 1, we show the Raman spectra of metal-free ($r = 0$) and Cu(II)-bound ($r =$ 0.5 and 1.0) PHGGG in D_2O solution. In the spectrum of metal-free PHGGG (Figure 1D), the $C_4{=}C_5$ stretch band of N-deuterated histidine appears at 1568 cm^{-1}, and this singlet band upshifts to 1584 cm^{-1} in the presence of Cu(II) (Figure 1, E and F). The imidazole ring breathing mode of N-deuterated histidine at 1272 cm^{-1} gains intensity with a small shift in peak position in the presence of Cu(II). The wavenumber upshift of the $C_4{=}C_5$ stretch band and the intensification of the ring breathing mode observed in D_2O solution support the binding of Cu(II) to the N_π atom of the histidyl imidazole ring. Strong sharp bands at 1502 and 1394 cm^{-1} in the D_2O solution spectra at $r = 0.5$ and 1.0 are also markers of N-deuterated histidine coordinating to a metal ion via the N_π atom (*19*, *21*).

Another spectral change associated with Cu(II) binding is seen at 1420 cm^{-1} (Figure 1). The Raman intensity at 1420 cm^{-1} increases with increase of *r* in both H_2O and D_2O solutions. On the other hand, the amide I band in H_2O (∼1665 cm^{-1}) and its counterpart in D_2O (amide I′, ∼1655 cm^{-1}) lose intensity. It is known that deprotonation of the amide group produces a strong band around 1420 cm^{-1} assignable to the in-phase stretch of the C=O/C−N^- bonds, and concomitantly the usual amide I band disappears (*22*). Thus, the intensity increase at 1420 cm^{-1} and the intensity decrease of the amide I (I′) band are ascribed to the deprotonation of amide nitrogen caused by the binding of Cu(II). In the D_2O solution spectra, the amide I′ band loses nearly half of its intensity at $r = 1.0$, indicating two out of four amide nitrogens of PHGGG are deprotonated in the Cu(II)−PHGGG complex. In previous papers (*16*, *19*), we reported Raman spectra of Cu(II) complexes of L-histydylglycylglycylglycine (HGGG) and L-histydylglycylglycine (HGG). A strong band due to deprotonated amide appeared at 1419 cm^{-1} in the spectrum of Cu(II)−HGGG, whereas no amide deprotonation was observed for Cu(II)−HGG. Accordingly, it is concluded that the triglycine segment of PHGGG plays a key role in the deprotonation and metal coordination of amide nitrogens. The above-mentioned spectral changes of PHGGG in both H_2O and D_2O solutions were observed only in the course of Cu(II) addition up to $r = 1.0$. Further addition of Cu(II) did not affect the Raman spectrum significantly (data not shown), indicating that PHGGG forms a 1:1 complex with Cu(II).

Raman Spectra of Cu(II)−OP1. Figure 3 shows the Raman spectra of H_2O (pH 8.2, left panel) and D_2O (pD 8.2, right panel) solutions of PHGGGWGQ (OP1) at Cu(II)/peptide

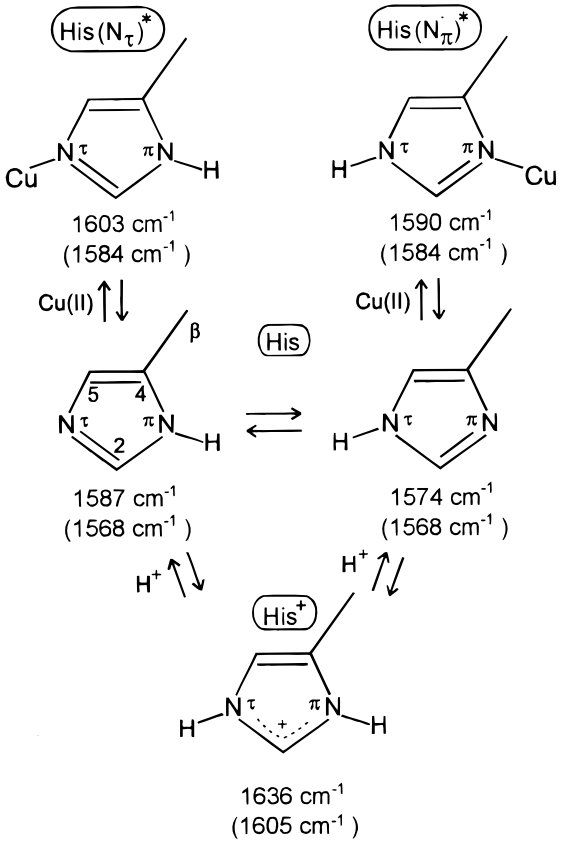

FIGURE 2: Protonation and metal-coordination dependence of the $C_4{=}C_5$ stretch wavenumber of histidine. The wavenumbers observed in this study are shown. His(N_τ)* and His(N_π)*, histidine coordinating to Cu(II) via N_τ or N_π, respectively (top); His, N_π- or N_τ-protonated tautomeric form of neutral histidine (middle); His^+, histidinium (bottom). The wavenumbers in parentheses are in D_2O solution.

molar ratios (*r*) of 0, 0.5, and 1.0. Most of the Raman bands in the spectra are ascribed to tryptophan side chain vibrations as indicated with the mode labels W1−W10 (*23*). Histidine Raman bands are covered by tryptophan bands in the absence of Cu(II) (Figure 3A). For example, the $C_4{=}C_5$ stretch of metal-free histidine, which was observed in the Raman spectrum of PHGGG as a doublet at 1587/1574 cm^{-1} (Figure 1A), is not seen in the spectrum of OP1 due to the overlap of the stronger W2 band at 1577 cm^{-1}. In the presence of Cu(II), however, a weak band assignable to the $C_4{=}C_5$ stretch of metal-bound histidine appears at 1590 cm^{-1}, and its intensity increases on going from $r = 0.5$ to 1.0 (Figure 3, B and C). Concomitantly, the 1577 cm^{-1} band becomes weaker, probably reflecting an upshift of the underlying $C_4{=}C_5$ stretch band of histidine from ∼1575 to 1590 cm^{-1}. The ring breathing band of metal-bound histidine also becomes detectable at 1274 cm^{-1} in the spectrum at $r = 0.5$ (Figure 3B), and it further gains intensity at $r = 1.0$ (Figure 3C). These Raman spectral features suggest that the histidine residue of OP1 binds to Cu(II) via the N_π atom.

The Cu(II)−His(N_π) binding of OP1 is confirmed by the Raman spectra in D_2O solution (Figure 3, right panel). The 1571 cm^{-1} band in the spectrum at $r = 0$ (Figure 3D) is assignable to an overlap of the W2 band of N-deuterated tryptophan and the $C_4{=}C_5$ stretch band of N-deuterated histidine. In the presence of Cu(II), a shoulder becomes detectable at 1584 cm^{-1}, and its intensity increases with increase of the concentration of Cu(II) from $r = 0.5$ to 1.0 (Figure 3, E and F). The 1584 cm^{-1} band is a marker of metal−histidine coordination as described above. The ring breathing mode of N-deuterated histidine at 1268 cm^{-1} shows an intensity increase characteristic of metal−His(N_π) binding (Figure 3, E and F). The 1502 cm^{-1} band of N_τ-deuterated, N_π−metal-ligated histidine becomes prominent at $r = 1.0$. These spectral changes are all consistent with Cu(II)−His-(N_π) binding.

The intensity at 1420 cm^{-1} slightly increases on going from $r = 0$ to $r = 1.0$ in the Raman spectra of H_2O solution of OP1 (Figure 3, B and C), suggesting an emergence of the in-phase C═O/C−N^- stretch band of deprotonated amide in the presence of Cu(II). This is more clearly seen in D_2O solution spectra because the W6 band of tryptophan shifts from the 1420 cm^{-1} region to 1384 cm^{-1} on deuteration of the indole nitrogen and does not overlap the C═O/C−N^- stretch band (Figure 3, E and F). The intensity increase of the 1420 cm^{-1} band is accompanied by an intensity decrease of the amide I (I′) band. At $r = 1.0$, the intensity of the amide I′ band decreases by 30% compared to that at $r = 0$, which indicates that about two of the seven amide groups of OP1 deprotonate in the 1:1 Cu(II)−OP1 complex. The deprotonated amide groups are likely to be in the triglycine segment as was in the case of the Cu(II)−PHGGG complex. The Raman spectra strongly suggest that two deprotonated amide nitrogens of the triglycine segment together with the histidyl N_π atom bind to a Cu(II) ion in the Cu(II)−OP1 complex.

Raman Spectra of Cu(II)−OP2 and Cu(II)−OP4. Figure 4 shows the Raman spectra of the octapeptide repeat OP2 ($r = 0$) and its Cu(II) complexes ($r = 0.5$ and 1.0) in H_2O (pH 8.2, left panel) and D_2O (pD 8.2, right panel) solutions. Note that the *r* value represents the molar ratio of Cu(II) to the octapeptide unit and therefore the Cu(II)/OP2 molar ratio is given by twice the value of *r*. The Raman spectra of OP2 in both H_2O and D_2O solutions exhibit a Cu(II) concentration dependence similar to that observed for OP1, i.e., a wavenumber upshift of the $C_4{=}C_5$ stretch (to 1590 and 1584 cm^{-1} in H_2O and D_2O, respectively) and an intensity increase of the imidazole ring breathing mode (at 1277 and 1268 cm^{-1} in H_2O and D_2O, respectively) together with an intensity increase of the C═O/C−N^- stretch band (1420 cm^{-1}) accompanied by a decrease of the amide I (I′) band intensity. The close similarity of Raman spectra between the Cu(II)−OP1 and C(II)−OP2 complexes suggests that each octapeptide unit of OP2 almost independently forms a Cu(II) complex, whose structure is analogous to that of the Cu-(II)−OP1 complex. Only one difference between the Cu-(II)−OP1 and Cu(II)−OP2 complexes is seen in the D_2O solution spectra at $r = 1.0$. The 1420 cm^{-1} amide$^-$ band of Cu(II)−OP2 is a little stronger than that of Cu(II)−OP1 (compare Figures 3F and 4F). Probably, at high concentrations of Cu(II), OP2 forms a minor complex, in which additional amide nitrogens deprotonate and coordinate to Cu-(II).

We have also examined Raman spectra of OP4 in the presence of Cu(II). The general features of the Raman spectrum of Cu(II)−OP4 at $r = 1.0$ (Figure 5) are similar to those of Cu(II)−OP1 (Figure 3), indicating that each octapeptide unit of OP4 forms a 1:1 complex with Cu(II)

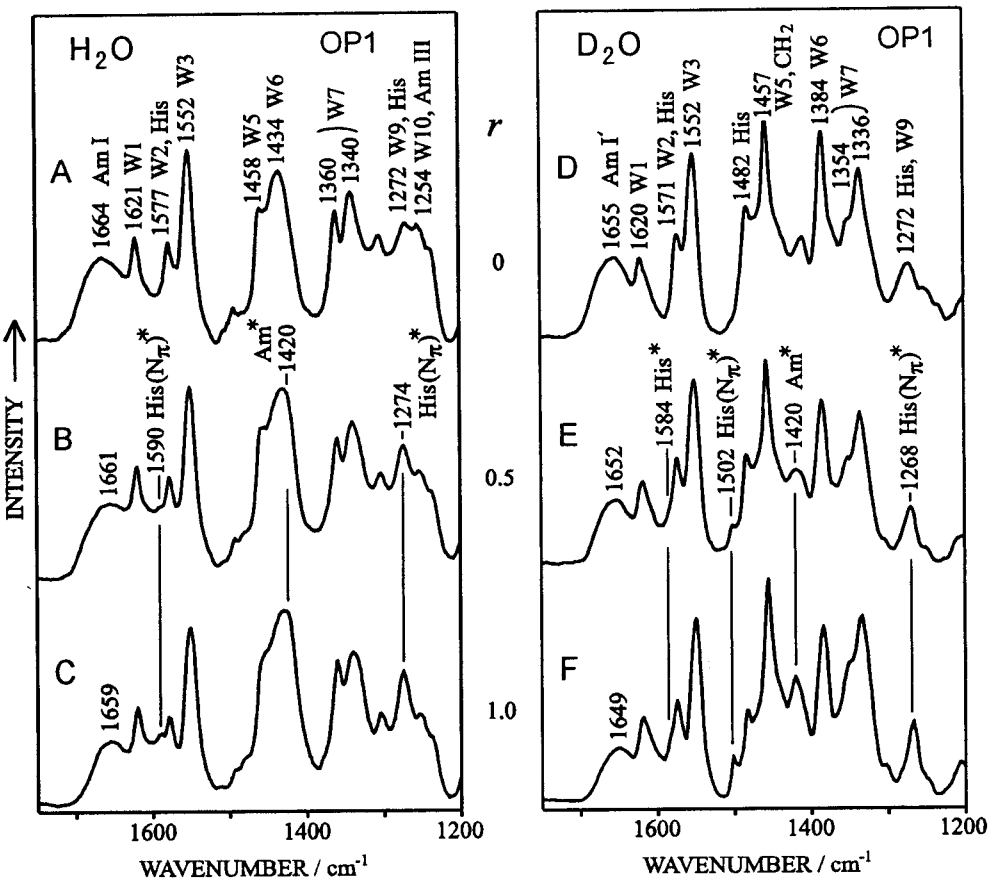

FIGURE 3: Raman spectra of H_2O (left panel) and D_2O (right panel) solutions of OP1 [20 mM, pH (pD) 8.2] at varied $CuCl_2$ concentrations. The molar concentration ratios of the Cu(II) ion to the octapeptide unit (r) are 0 (A and D), 0.5 (B and E), and 1.0 (C and F). The Raman intensity was normalized by using the 1552 cm^{-1} tryptophan band (W3). Solvent Raman bands were subtracted. Tryptophan Raman bands are labeled with W1−W10. For the designations of the other Raman bands, see the caption to Figure 1.

analogous to that formed by OP1. A noticeable difference between the OP1 and OP4 spectra is the appearance of a new weak band at 1287 cm^{-1} in the D_2O solution of Cu(II)−OP4 ($r = 1.0$). This weak Raman band is assignable to metal-bridging imidazolate (*21*) and suggests that some of the histidine residues of OP4 are coordinating to Cu(II) ions via both N_π and N_τ. Additionally, the intensity ratio of the 1360/1340 cm^{-1} doublet (W7) of tryptophan is higher at $r = 1.0$ than at $r = 0$ (Figure 5, left panel). Since the W7 intensity ratio increases with increase in environmental hydrophobicity of the tryptophan indole ring (*24*, *25*), the tryptophan side chain may not be fully exposed to the solvent water in the Cu(II)−OP4 complex. Probably, the long peptide chain of Cu(II)−OP4 takes major extended and minor folded forms. In the extended form, each octapeptide unit independently binds one Cu(II) ion, whereas in the folded form the Cu(II)-coordinated octapeptide units interact with each other through Cu(II)−His−Cu(II) bridges with the tryptophan side chains buried inside the folded peptide.

Absorption Spectra. In Cu(II) complexes of peptides, the Cu(II) ion is usually coordinated by four equatorial ligands in a tetragonal geometry (*26*). Additional ligands in the axial positions are generally water molecules in aqueous solution, but in some cases they are weakly bound ligand atoms. The λ_{max} of the Cu(II) d−d transition is mainly determined by the strength of the ligand field, in particular of the equatorial ligands (*27*, *28*). Water and the carbonyl group are weak ligands. Substitution of a weak ligand to a strong one such as carboxylate, imidazole, amino, or deprotonated amide causes a blue shift of about 20, 45, 50, or 60 nm, respectively, when the original λ_{max} is located around 600 nm (*27*). On the other hand, apical coordination of a strong ligand causes a red shift of about 40 nm (29). Thus, a change of ligand is expected to result in a significant shift of the d−d transition.

Figure 6 shows visible absorption spectra in the d−d transition region of the Cu(II) complexes of PHGGG, OP1, OP2, and OP4. In recording these spectra, the peptide concentration was kept constant, and varied amounts of Cu(II) were added. The λ_{max} of the d−d transition of Cu(II)−PHGGG is located at 623 nm, and it does not change with the concentration of Cu(II) (Figure 6A). The intensity of the d−d absorption reaches a plateau at $r = 1.3$. These observations indicate that Cu(II) binds to PHGGG in a single 1:1 form. Taken together with the Raman data reported above, the N_π atom of histidine and two deprotonated amide nitrogens in the triglycine segment are considered to be the equatorial ligands in the Cu(II)−PHGGG complex. The fourth equatorial ligand may be a water molecule. The λ_{max} of Cu(II)−PHGGG is close to the value (610 nm) reported for a ternary complex of Cu(II), glycylglycine, and imidazole, in which the Cu(II) ion is coordinated by the α-amino and amide nitrogens of glycylglycine together with one imidazole nitrogen (*29*).

For the Cu(II)−OP1 complex (Figure 6B), the d−d transition is observed at 615 nm, and the λ_{max} is again insensitive to the Cu(II) concentration. Since the λ_{max} of the Cu(II)−OP1 complex is close to that of Cu(II)−PHGGG, the equatorial ligands in Cu(II)−OP1 must be the same as

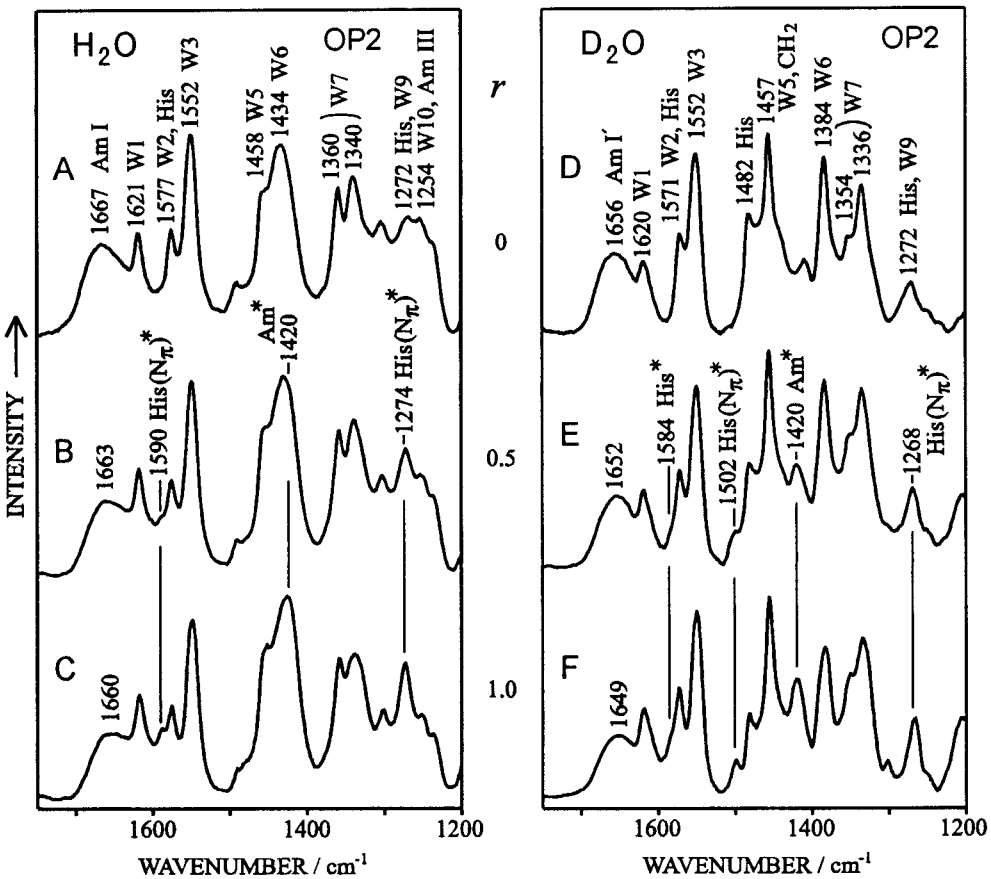

FIGURE 4: Raman spectra of H_2O (left panel) and D_2O (right panel) solutions of OP2 [20 mM in octapeptide unit, pH (pD) 8.2] at varied $CuCl_2$ concentrations. The molar concentration ratios of the Cu(II) ion versus the octapeptide unit (r) are 0 (A and D), 0.5 (B and E), and 1.0 (C and F). The Raman intensity was normalized by using the 1552 cm^{-1} tryptophan band (W3). Raman scattering from the solvent was subtracted. The designations of Raman bands are the same as in Figure 3.

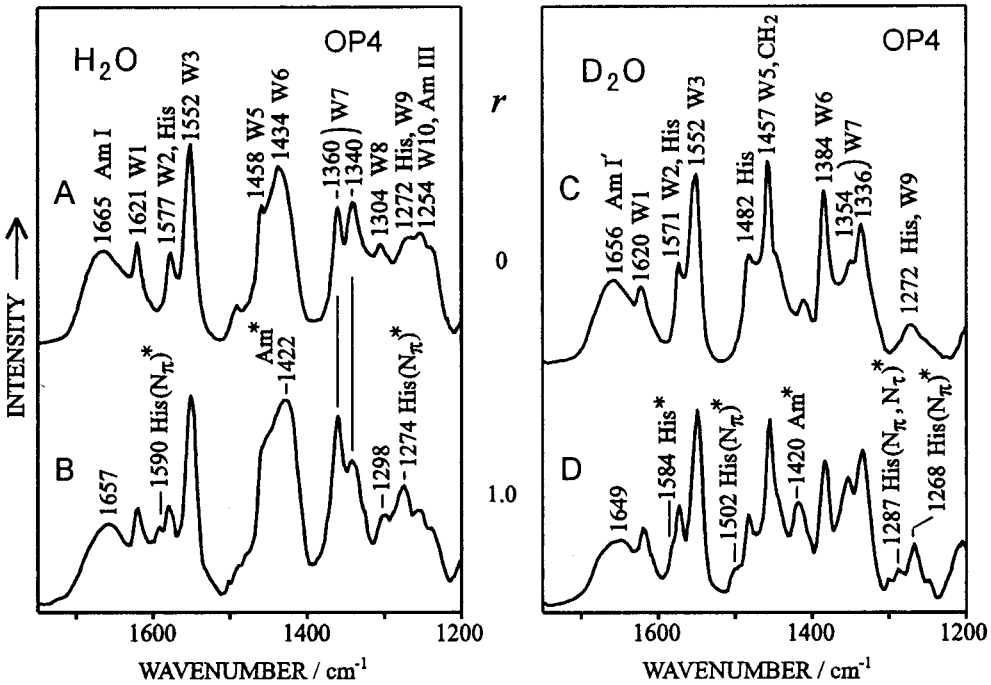

FIGURE 5: Raman spectra of H_2O (left panel) and D_2O (right panel) solutions of OP4 [20 mM in octapeptide unit, pH (pD) 8.2] in the absence ($r = 0$, A and C) and presence ($r = 1.0$, B and D) of Cu(II). The Raman intensity was normalized by using the 1552 cm^{-1} tryptophan band (W3). Raman scattering from the solvent was subtracted. The Raman band of metal-bridging imidazolate is denoted with His (N_π, N_τ)*. For the designations of the other Raman bands, see the caption to Figure 3.

those in Cu(II)−PHGGG. The small difference in λ_{max} between PHGGG (623 nm) and OP1 (615 nm) may be attributed to a difference in coordination geometry or in apical ligand.

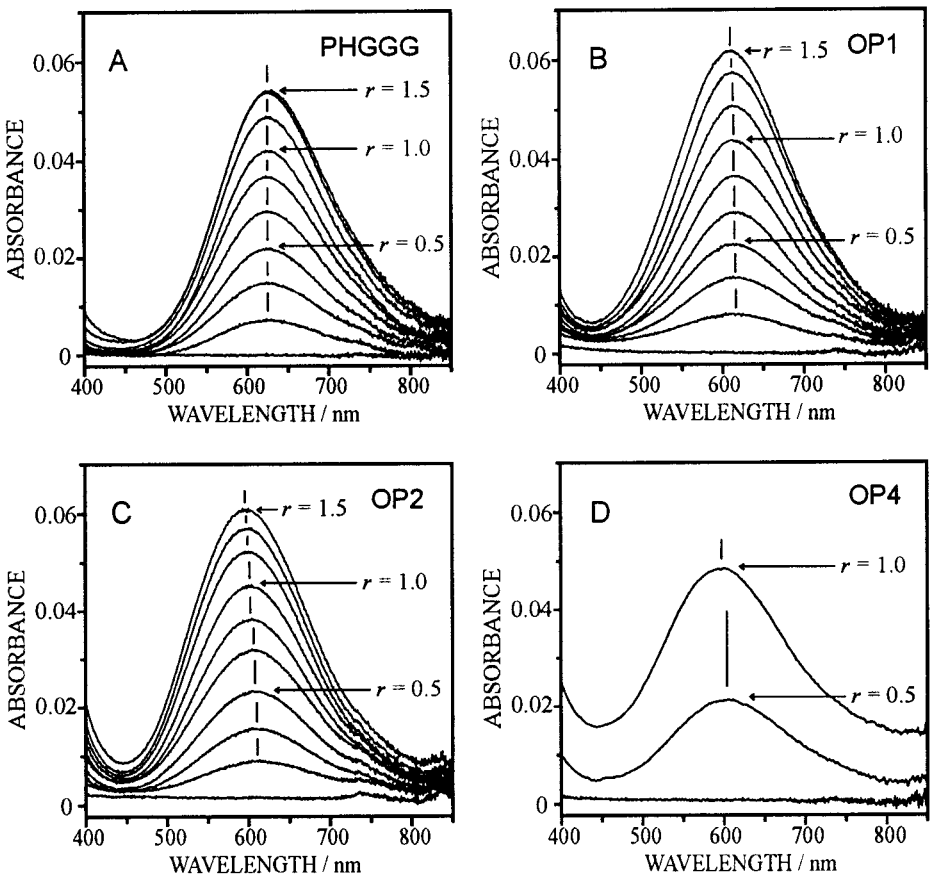

FIGURE 6: Visible absorption spectra of Cu(II)−PHGGG (A), Cu(II)−OP1 (B), Cu(II)−OP2 (C), and Cu(II)−OP4 (D) at a constant peptide concentration (120 μM in pentapeptide or octapeptide unit) and varied $CuCl_2$ concentrations (0, 20, 40, 60, 80, 100, 120, 140, 160, and 180 μM from bottom to top in A−C and 0, 60, and 120 μM in D). A cell of 5-cm path length was used. The vertical lines indicate the positions of λ_{max}.

The λ_{max} of the Cu(II)−OP2 complex depends on the concentration of Cu(II). It changes from 613−610 to 599−597 nm with a transition midpoint at $r = 1.0$ (Figure 6C). Below $r = 1.0$, the λ_{max} is nearly identical to that of the Cu(II)−OP1 complex, while it is significantly blue-shifted above $r = 1.0$. At low concentrations of Cu(II), each octapeptide unit of OP2 may independently form a complex with Cu(II), whose structure is very similar to that of Cu(II)−OP1. In the presence of excess amounts of Cu(II), on the other hand, Cu(II) may bind to additional sites of the peptide such as WGQPH in the joint region of the two octapeptide units in OP2. The additional amide deprotonation of OP2 at high Cu(II) concentrations has been suggested by Raman spectroscopy as described above.

We have also investigated visible absorption spectra of OP4 in the presence of Cu(II) (Figure 6D). The λ_{max} of the d−d transition was found at 607 and 600 nm at $r = 0.5$ and 1.0, respectively. At higher concentrations of Cu(II), the complex precipitated. The λ_{max} values are close to those observed for the Cu(II)−OP2 complex, indicating that the primary equatorial ligands to Cu(II) are the same as in the Cu(II) complexes of the other peptides described above. Partial aggregation of the peptide is suggested by the rise of base line at $r = 1.0$, and the intermolecular association may be a cause of the blue shift from 607 nm at $r = 0.5$ to 600 nm at $r = 1.0$.

pH Dependence of Cu(II)−OP2 Complexation. Figure 7 shows the Raman spectra of H_2O (left panel) and D_2O (right panel) solutions of OP2 (10 mM in peptide, 20 mM in octapeptide unit) at pH (pD) from 8.8 (top) to 4.0 (bottom) in the presence of 20 mM Cu(II) ($r = 1.0$). Exceptionally, the spectra at pH 6.0 and pD 6.0 were obtained from the precipitates because the Cu(II)−OP2 complex was insoluble at this pH (pD) as described under Experimental Procedures. The Raman spectra of Cu(II)−OP2 at pH (pD) 8.8, 7.4, and 6.4 bear strong resemblance with that at pH (pD) 8.2 (compare Figures 4 and 7), indicating that the structure of the Cu(II)−OP2 complex remains unchanged above pH 6.4. The involvement of deprotonated amide nitrogens in Cu(II) coordination is evidenced by the appearance of the 1420 cm^{-1} amide band. The Cu(II)−histidine binding via the N_π atom is confirmed by the $C_4{=}C_5$ stretch band at 1590 cm^{-1} and the strong imidazole ring breathing band at 1274 cm^{-1} (1268 cm^{-1} in D_2O). The 1502 cm^{-1} band characteristic of N_π−metal coordination is also prominent in the D_2O solution spectra at pD $\geq$ 6.4.

In contrast, the Raman spectrum at pH (pD) 6.0 differs significantly from those at higher pH in the respect that it lacks the marker bands of the deprotonated amide and of the N_π coordination of histidine. The absence of the 1420 cm^{-1} band indicates that amide groups are not involved in Cu(II) coordination. The complete dissociation of Cu(II) and concomitant protonation at the amide nitrogens take place in a narrow pH range from 6.4 to 6.0. Analogous sharp and cooperative transitions of metal binding/unbinding at multiple amide sites have been reported for peptides containing glycine and histidine (*31*). The significant intensity decrease

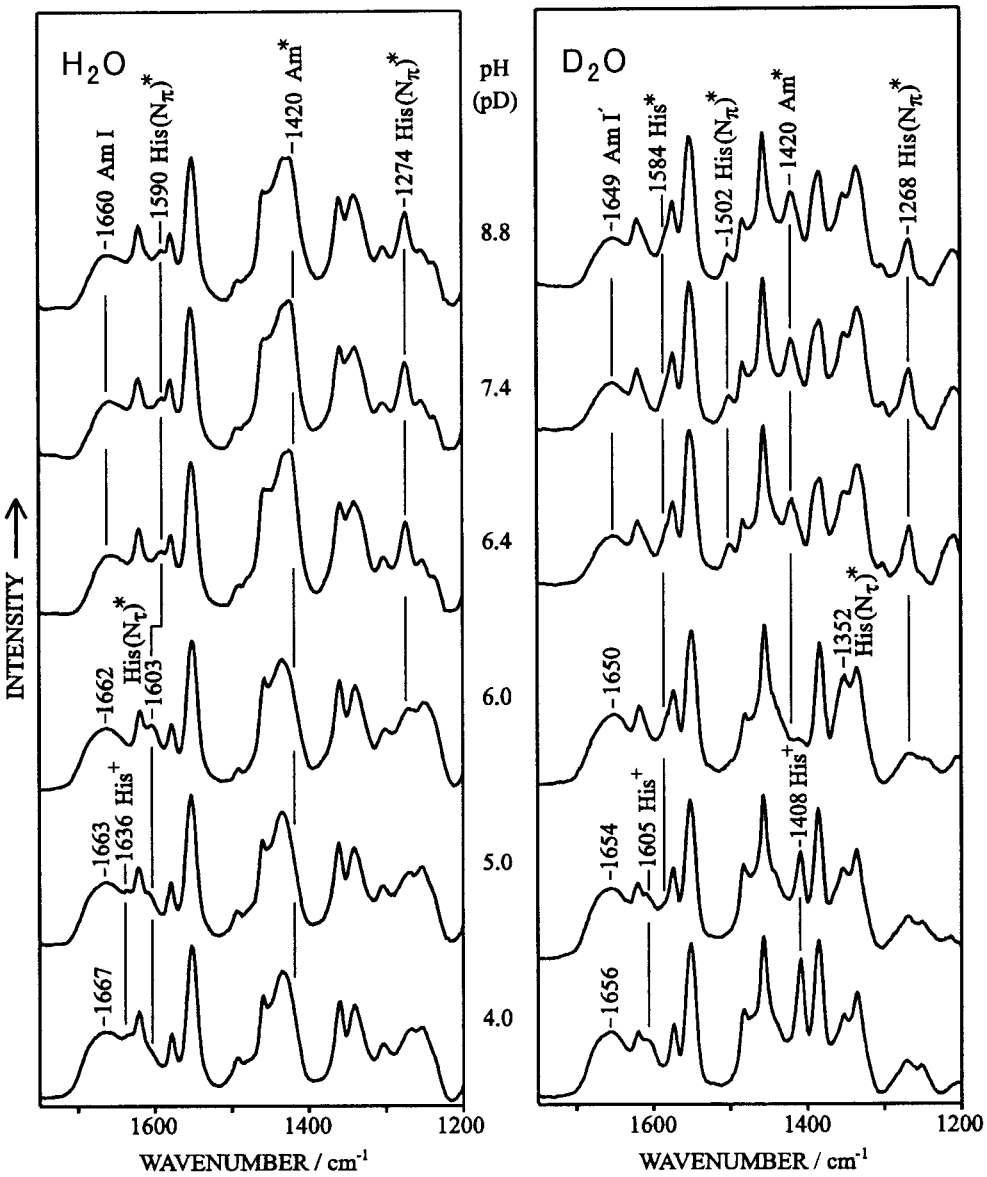

FIGURE 7: Raman spectra of H_2O (left panel) and D_2O (right panel) solutions of OP2 (20 mM in octapeptide unit) in the presence of Cu(II) ($r = 1.0$) at varied pH (pD): 8.8, 7.4, 6.4, 6.0, 5.0, and 4.0 from top to bottom. The Raman intensity was normalized by using the 1552 cm^{-1} tryptophan band (W3). Solvent Raman bands were subtracted. His(N_τ)* and His^+ denote the Raman bands of histidine bound to Cu(II) via the N_τ atom and of histidinium, respectively. For the designations of the other Raman bands, see the caption to Figure 3.

of the imidazole ring breathing mode (1274 cm^{-1} in H_2O and 1268 cm^{-1} in D_2O) and the disappearance of the 1502 cm^{-1} band in D_2O solution provide evidence that the N_π atom of histidine does not act as a ligand any more. Instead, the appearance of a new band at 1603 cm^{-1} (in H_2O) indicates that the N_τ atom (not the N_π atom) of histidine coordinates to Cu(II) at pH 6.0 (*19*) (Figure 2). An intensity increase at 1352 cm^{-1} in the pD 6.0 spectrum is also consistent with the N_τ−Cu(II) coordination of histidine, because a histidine Raman band around 1350 cm^{-1} gains intensity upon N_τ−metal coordination in D_2O (*19*, *21*). As described above, the C_4═C_5 stretch of N-deuterated histidine exhibits a wavenumber upshift from 1568 to 1584 cm^{-1} on metal binding to either the N_π or the N_τ atom. The 1584 cm^{-1} shoulder band at pD 8.8−6.4 remains unchanged at pD 6.0, which confirms that the Cu(II)−histidine binding persists at pH (pD) 6.0, though the site of ligation is changed from N_π to N_τ. The switch of the Cu(II) binding site on the imidazole ring of histidine is synchronized with the dissociation of Cu(II) from the amide nitrogens. This observation strongly suggests that the Cu(II)−His(N_π) coordination in the 1:1 Cu(II)−octapeptide complex at basic or neutral pH is stabilized by the additional coordination of the adjacent amide groups to the same Cu(II) ion.

At pH 5.0 and 4.0, no indication of amide deprotonation is observed as was at pH 6.0. The marker of N_τ−metal coordination of histidine at 1603 cm^{-1} becomes less intense as the pH decreases from 6.0 to 4.0 (Figure 7, left panel). Concomitant with this intensity decrease, an intensity increase is seen at 1636 cm^{-1}. Likewise, the shoulder band at 1584 cm^{-1} disappears, and a new band emerges at 1605 cm^{-1} on going from pD 6.0 to 5.0 in D_2O solution (Figure 7, right panel). The newly observed bands are ascribed to the C_4═C_5 stretch of histidinium, both N_π and N_τ being protonated or deuterated (*31*) (Figure 2). The N_π−C_2−N_τ symmetric stretch mode of N-deuterated histidinium gives a sharp characteristic band at 1408 cm^{-1} in the spectra at pD 5.0 and 4.0 (*31*). Under highly acidic conditions, both

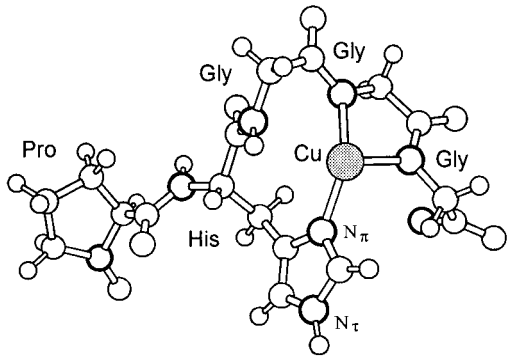

FIGURE 8: Model for the Cu(II) binding mode of the octapeptide unit PHGGGWGQ at neutral and basic pH. Only the C(II)-bound PHGGG segment is shown. The Cu(II) ion is shaded, and the nitrogen atoms are drawn with thick open circles. The PHGGG segment binds a Cu(II) ion via the histidyl N_π atom and the deprotonated amide nitrogens of the second and third glycine residues. The fourth ligand of the Cu(II) ion may be a water molecule in OP1, OP2, and the extended form of OP4, while it may be the histidyl N_τ atom of another octapeptide unit in the folded form of OP4.

N_π and N_τ of histidine are protonated, and this inhibits Cu(II)−histidine binding.

The change of the Cu(II) binding mode associated with the pH change may be related to the strong pH dependence of peptide solubility described under Experimental Procedures. Above pH 6.4, the Cu(II) is coordinated by a histidine N_π and two amide nitrogens, and the Cu(II) complex is more or less soluble. However, the complex becomes almost insoluble at pH 6.0, where the histidine side chain provides metal coordination site (N_τ) but the main chain amide does not. The peptide again becomes soluble upon breakage of the Cu(II)−His(N_τ) bond at pH $\leq$5.0. These observations suggest that the large decrease of peptide solubility around pH 6.0 reflects an aggregation of the peptide caused by intermolecular cross-linking through His(N_τ)−Cu(II)−His(N_τ) bridges. The involvement of two histidines, i.e., two octapeptide units, in the coordination to a Cu(II) ion is supported by the observation that the same precipitation occurred even at $r = 0.5$ and the precipitate at $r = 0.5$ gave a Raman spectrum identical to that obtained from the precipitate at $r = 1.0$ (data not show). The switch of the metal binding site of histidine from N_π to N_τ in the aggregate at pH 6.0 may be explained by assuming that the N_τ atom, is are located at a longer distance from the peptide main chain than N_π, is easier to share a Cu(II) ion with another N_τ atom of a different peptide chain.

DISCUSSION

The Raman and absorption spectra reported here have shown that each unit in tandem repeats of the octapeptide PHGGGWGQ binds a Cu(II) ion via the N_π atom of the histidine side chain and two deprotonated amide nitrogens in the triglycine segment at neutral or basic pH. We have built a possible molecular model for the 1:1 Cu(II)−octapeptide complex on the basis of the present spectral data (Figure 8). In the model, the histidyl N_π atom and the deprotonated amide nitrogens of the second and third glycine residues occupy three of the four tetragonal ligand positions. PrP contains a tandem repeat of four octapeptide units in the N-terminal region, and the octapeptide repeat region is believed to be the binding site of Cu(II) (*13*−*16*). It is interesting to discuss whether the Cu(II) binding mode of the octapeptide unit revealed here is applicable to the octapeptide repeat region in the protein PrP.

In proteins, the main-chain amide is usually neutral because of its very weak acidity ($pK_a \approx 15$) (*28*). However, ionization of the amide group is promoted in the presence of Cu(II) when a histidine residue and the N-terminal amino group are available as primary ligating sites (*30*). Such Cu(II) complexes are formed at the N-termini of serum albumins and with short peptides that mimic the Cu(II) binding sites of albumins (e.g., glycylglycyl-L-histidine) (*28*, *32*, *33*). Amide deprotonation also occurs in Cu(II) complexes of peptides such as acetylglycylglycyl-L-histidine (*34*), which has only one primary ligating site. This suggests that Cu(II) binding to a histidine side chain even in the interior of a protein may induce ionization of amide groups nearby. A possible factor against such a chelation is steric hindrance caused by amino acid side chains and the peptide backbone, because metal chelation requires a compact arrangement of the primary ligation site and amide nitrogens (*30*, *35*). The PrP octapeptide contains a highly flexible glycine-rich region adjacent to the primary ligating site (histidine); thereby, the steric problem may be solved in PrP. The Cu(II) binding mode of the octapeptide unit revealed here is likely to be applicable to the octapeptide repeat region in PrP.

An equilibrium dialysis study on the entire N-terminal domain of human PrP suggested 5.6 ($\pm$0.4) Cu(II) binding sites per protein (*15*). Another equilibrium dialysis study on the full-length PrP from Syrian hamster showed saturation of the protein by Cu(II) at about 2 mol equiv of Cu(II) (*14*). Both human and hamster PrPs contain a tandem repeat of four octapeptide units with an analogous nonapeptide on the adjacent N-terminal side. The discrepancy between the two dialysis studies could be due to a difference in pH. The former equilibrium dialysis was carried out at pH 7.4, whereas the latter was at pH 6.0. The present Raman study has shown that each octapeptide unit can form a 1:1 Cu(II)−octapeptide complex at neutral or basic pH, which is consistent with the result of the former dialysis study at pH 7.4 (*15*), if an additional Cu(II) ion binds to the nonapeptide region as well. At pH 6.0, on the other hand, the Cu(II)−amide$^-$ bonds dissociate, and only the histidine residues provide metal coordination sites. This change of the binding mode causes significant aggregation of the peptide attributable to the formation of intermolecular His−Cu−His bridges. The intermolecular association may partly be due to the high peptide concentration (20 mM in octapeptide units) in the Raman samples. In highly diluted solutions as employed in dialysis experiments, however, histidine side chains could form, at least partly, intramolecular His−Cu−His bridges with one Cu(II) ion shared by two histidines of adjacent octapeptide units. In any case, the number of Cu(II) binding sites per octapeptide is reduced to half at pH 6.0, and this is consistent with the result of the latter dialysis study at pH 6.0. (*14*). The pH dependence of the Cu(II) binding mode of PrP may be related to the physiological function of the protein.

The content of Cu in the brains of PrP^C gene-ablated ($Prnp^{0/0}$) mice is greatly reduced compared to those in wild-type mouse brains (*15*). The activity of a Cu(II)-dependent enzyme, superoxide dismutase, is also reduced in the $Prnp^{0/0}$

mouse brain (*36*). These findings indicate that PrP plays a role in regulating the intracellular Cu concentration in the brain. PrP is a glycolipid-anchored surface protein and is recycled between the plasma membrane and endosomal compartment (*37*). On the plasma membrane surface, the neutral extracellular medium may allow each of the four octapeptide units in PrP to accommodate one Cu(II) ion. In acidified endocytic compartments, however, the Cu(II)−amide$^-$ bonds would dissociate, and the affinity of PrP to Cu(II) would be reduced significantly, resulting in a release of Cu(II) ions. The pH-dependent affinity change is expected to play a role in internalizing extracellular Cu(II) ions and in regulating the Cu(II) concentration in brain cells.

PrP is also known as the infectious agent of transmissible spongiform encephalopathies including Creutzfeldt−Jakob disease (*1*, *5*, *6*). In infected cells, normal cellular prion protein (PrP^C) is converted to the protease-resistant pathogenic form (PrP^{Sc}) with a change in secondary structure from α-helix to *β*-sheet (*38*−*40*). Like other membrane glycoproteins, PrP^C is transported to lysosomes for degradation (*41*) during recycling between the plasma membrane and endosomal compartment (*36*). Although the mechanism of $PrP^C \rightarrow PrP^{Sc}$ conversion is not yet clarified, it is evidenced that PrP^{Sc} is formed prior to the entry into lysosomes (*42*) and PrP^{Sc} aggregates mainly in secondary lysosomes (*43*) with acquiring protease resistance before exposure to lysosomal proteases (*44*). Recently, Stöckel et al. have found that binding of Cu(II) promotes the conformational shift of PrP from a soluble α-helical to an insoluble *β*-sheet-rich structure (*14*). This result suggests that Cu(II) ions take part in the $PrP^C \rightarrow PrP^{Sc}$ conversion. In weakly acidic endosomal compartments, Cu(II) would dissociate from the amides in the octapeptide region of PrP^C, and the protein would form intermolecular His−Cu−His bridges. If such a cross-link of PrP^C molecules occurs in the N-terminal region, it may raise the probability of protein−protein contact also in the C-terminal region, which is considered to be important for the conversion of PrP^C into PrP^{Sc} (*45*).

REFERENCES

1. Prusiner, S. B. (1991) *Science 252*, 1515−1522.
2. Mobley, W. C., Neve, R. L., Prusiner, S. B., and McKinley, M. P. (1988) *Proc. Natl. Acad. Sci. U.S.A. 85*, 9811−9815.
3. Sakaguchi, S., Katamine, S., Nishida, N., Moriuchi, R., Shigematsu, K., Sugimoto, T., Nakatani, A., Kataoka, Y., Houtani, T., Shirabe, S., Okada, H., Hasegawa, S., Miyamoto, T., and Noda, T. (1996) *Nature 380*, 528−531.
4. Tobler, I., Gaus, S. E., Deboer, T., Achermann, P., Ficher, M., Rülicke, T., Moser, M., Oesch, B., McBride, P. A., and Manson, J. C. (1996) *Nature 380*, 639−642.
5. Prusiner, S. B. (1997) *Science 278*, 245−251.
6. Prusiner, S. B. (1998) *Proc. Natl. Acad. Sci. U.S.A. 95*, 13363−13383.
7. Liao, Y.-C., Lebo, R. V., Clawson, G. A., and Smuckler, E. A. (1986) *Science 233*, 364−367.
8. Turk, E., Teplow, D. B., Hood, L. E., and Prusiner, S. B. (1988) *Eur. J. Biochem. 176*, 21−30.
9. Huang, Z., Gabriel, J.-M., Baldwin, M. A., Fletterick, R., Prusiner, S. B., and Cohen, F. E. (1994) *Proc. Natl. Acad. Sci. U.S.A. 91*, 7139−7143.
10. Riek, R., Hornemann, S., Wider, G., Glockshuber, R., and Wüthrich, K. (1997) *FEBS Lett. 413*, 282−288.
11. Donne, D. G., Viles, J. H., Groth, D., Mehlhorn, I., James, T. L., Cohen, F. E., Prusiner, S. B., Wright, P. E., and Dyson, H. J. (1997) *Proc. Natl. Acad. Sci. U.S.A. 94*, 13452−13457.
12. Goldmann, W., Hunter, N., Martin, T., Dawson, M., and Hope, J. (1991) *J. Gen. Virol.*, 201−204.
13. Hornshaw, M. P., McDermott, J. R., and Candy, J. M. (1995). *Biochem. Biophys. Res. Commun. 207*, 621−629.
14. Stöckel, J., Safar, J., Wallace, A. C., Cohen, F. E., and Prusiner, S. B. (1998) *Biochemistry 37*, 7185−7193.
15. Brown, D. R., Qin, K., Herms, J. W., Madlung, A., Manson, J., Strome, R., Fraser, P. E., Kruck, T., von Bohlen, A., Schulz-Schaeffer, W., Giese, A., Westaway, D., and Kretzschmar, H. (1997) *Nature 390*, 684−687.
16. Miura, T., Hori-i, A., and Takeuchi, H. (1996) *FEBS Lett. 396*, 248−252.
17. Viles, J. H., Cohen, F. E., Prusiner, S. B., Goodin, D. B., Wright, P. E., and Dyson, H. J. (1999) *Proc. Natl, Acad. Sci. U.S.A. 96*, 2042−2047.
18. Ashikawa, I., and Itoh, K. (1979) *Biopolymers 18*, 1859−1876.
19. Miura, T., Satoh, T., Hori-i, A., and Takeuchi, H. (1998) *J. Raman Spectrosc. 29*, 41−47.
20. Miura, T., Satoh, T., and Takeuchi, H. (1998) *Biochim. Biophys. Acta 1384*, 171−179.
21. Hashimoto, S., Ono, K., and Takeuchi, H. (1998) *J. Raman Spectrosc. 29*, 969−975.
22. Tasumi, M. (1979) in *Infrared and Raman Spectroscopy of Biological Molecules* (Theophanides, T. M., Ed.) pp 225−240, D. Reidel Publishing Co., Dordrecht.
23. Harada, I., and Takeuchi, H. (1986) in *Spectroscopy of Biological Systems* (Clark, R. J. H., and Hester, R. E., Eds.) pp 113−175, Wiley, Chichester.
24. Harada, I., Miura, T., and Takeuchi, H. (1986) *Spectrochim. Acta 42A*, 307−312.
25. Miura, T., Takeuchi, H., and Harada, I. (1988) *Biochemistry 27*, 88−94.
26. Freeman, H. C. (1967) *Adv. Protein Chem. 22*, 257−424.
27. Billo, E. J. (1974) *Inorg. Nucl. Chem. Lett. 10*, 613−617.
28. Sigel, H., and Martin, B. (1982) *Chem. Rev. 82*, 385−426.
29. Koltun, W. L., Fried, M., and Gurd, F. R. N. (1960) *J. Am. Chem. Soc. 82*, 233−241.
30. Sundberg, R. J., and Martin, R. B. (1974) *Chem. Rev. 74*, 471−517.
31. Tasumi, M., Harada, I., Takamatsu, T., and Takahashi, S. (1982) *J. Raman Spectrosc. 12*, 149−151.
32. Sarkar, B., and Wigfield, Y. (1968) *Can. J. Biochem. 46*, 601−607.
33. Lau, S., Kruck, T. P. A., and Sarkar, B. (1974) *J. Biol. Chem. 249*, 5878−5884.
34. Bryce, G. F., Roeske, R. W., and Gurd, F. R. (1965) *J. Biol. Chem. 240*, 3837−3846.
35. Morris, P. J., and Martin, R. B. (1971) *Inorg. Chem. 10*, 964−970.
36. Brown, D. R., Schulz-Schaeffer, W. J., Schmidt, B., and Kretzschmar, H. A. (1997) *Exp. Neurol. 146*, 104−112.
37. Shyng, S., Huber, M. T., and Harris, D. A. (1993) *J. Biol. Chem. 268*, 15922−15928.
38. Pan, K.-M., Baldwin, M., Nguyen, J., Gasset, M., Serban, A., Groth, D., Mehlhorn, I., Huang, Z., Fletterick, R. J., Cohen, F. E., and Prusiner, S. B. (1993) *Proc. Natl. Acad. Sci. U.S.A. 90*, 10962−10966.
39. Nguyen, J., Baldwin, M. A., Cohen, F. E., and Prusiner, S. B. (1995) *Biochemistry 34*, 4186−4192.
40. Borchelt, D. R., Scott, M., Taraboulos, A., Stahl, N., and Prusiner, S. B. (1990) *J. Cell Biol. 110*, 743−752.
41. Caughey, B., Race, R. E., Ernst, D., Buchmeier, M. J., and Chesebro, B. (1989) *J. Virol. 63*, 175−181.
42. Borchelt, D. R., Taraboulos, A., and Prusiner, S. B. (1992) *J. Biol. Chem. 267*, 16188−16199.
43. McKinley, M. P., Meyer, R. K., Kenaga, L., Rahbar, F., Cotter, R., Serban, A., and Prusiner, S. B. (1991) *J. Virol. 65*, 1340−1351.
44. Taraboulos, A., Raeber, A., Borchelt, D. R., McKinley, M. P., and Prusiner, S. B. (1991) *FASEB J. 5*, A1177.
45. Come, J. H., Fraser, P. E., and Lansbury, P. T., Jr. (1993) *Proc. Natl. Acad. Sci. U.S.A. 90*, 5959−5963.

BI9909389